Electronic Supporting Information

An unprecedented formation of N-benzamidobisthiourea derivative and its PET promoted CT state specific towards fluoride ion

Ranganathan Koteeswari, Pichandi Ashokkumar, Vayalakkavoor T. Ramakrishnan,* E. J. Padma Malar and Perumal Ramamurthy*

Contents

Materials and methods

Dimedone, 4-carboxybenzaldehyde and all anions as their tetrabutyl ammonium salts were purchased from Sigma Aldrich Chemicals Pvt. Ltd. and were used as received. The solvent acetonitrile (HPLC grade) was purchased from Qualigens India Ltd. Absorption spectra were recorded on Agilent 8453 diode array spectrophotometer. Emission spectra were recorded on HORIBA JOBIN YVON Fluoromax 4P spectrophotometer. NMR spectra were recorded on Bruker Avance III 500 MHz and Bruker 300 MHz instruments in deuterated solvents as indicated; TMS or the residual solvent peaks were used as internal standards. Chemical shifts are reported in ppm and coupling constants ($J_{X\text{-}X'}$) are reported in Hz. ESI-MS were performed on an ECA LCQ Thermo system with ion-trap detection in positive and negative mode. Elemental analyses (C, H and N) were taken on a Euro EA Elemental analyzer. Fluorescence decays were recorded using TCSPC method as described elsewhere and femtosecond upconversion technique. In femto upconversion, the sample solution was excited with frequency doubled laser pulse (400 nm), generated by coupling FOG-100 (CDP, Russia) with a 60 fs Ti-sapphire Laser (Tsunami, Spectra Physics). The polarization of the excitation beam for magic angle condition was controlled with a Berek compensator. The rotating sample cuvette was 1 mm thick. The horizontally polarized fluorescence emitted from the sample was upconverted in a BBO crystal with residual IR gate pulse passing through a variable delay line with a resolution of 6.25 fs. Spectral resolution was achieved by dispersing the upconverted light in a spectrometer with single monochromator and a photon counter. The FOG-100 had a 350 fs (FWHM) cross correlation function and maximum time delay of 1.7 ns. The fluorescence decay curves were fitted with windows based LUMEX 3.1 software (CDP), and the quality of fit was judged from the χ^2 and residuals. Cyclic voltammograms were recorded using a CHI-620B Electrochemical Analyzer, CH Instruments Inc.

A platinum disc working electrode, non-aqueous Ag/AgCl reference electrode and platinum wire counter electrode were employed for the CV experiments.

Experimental Procedures

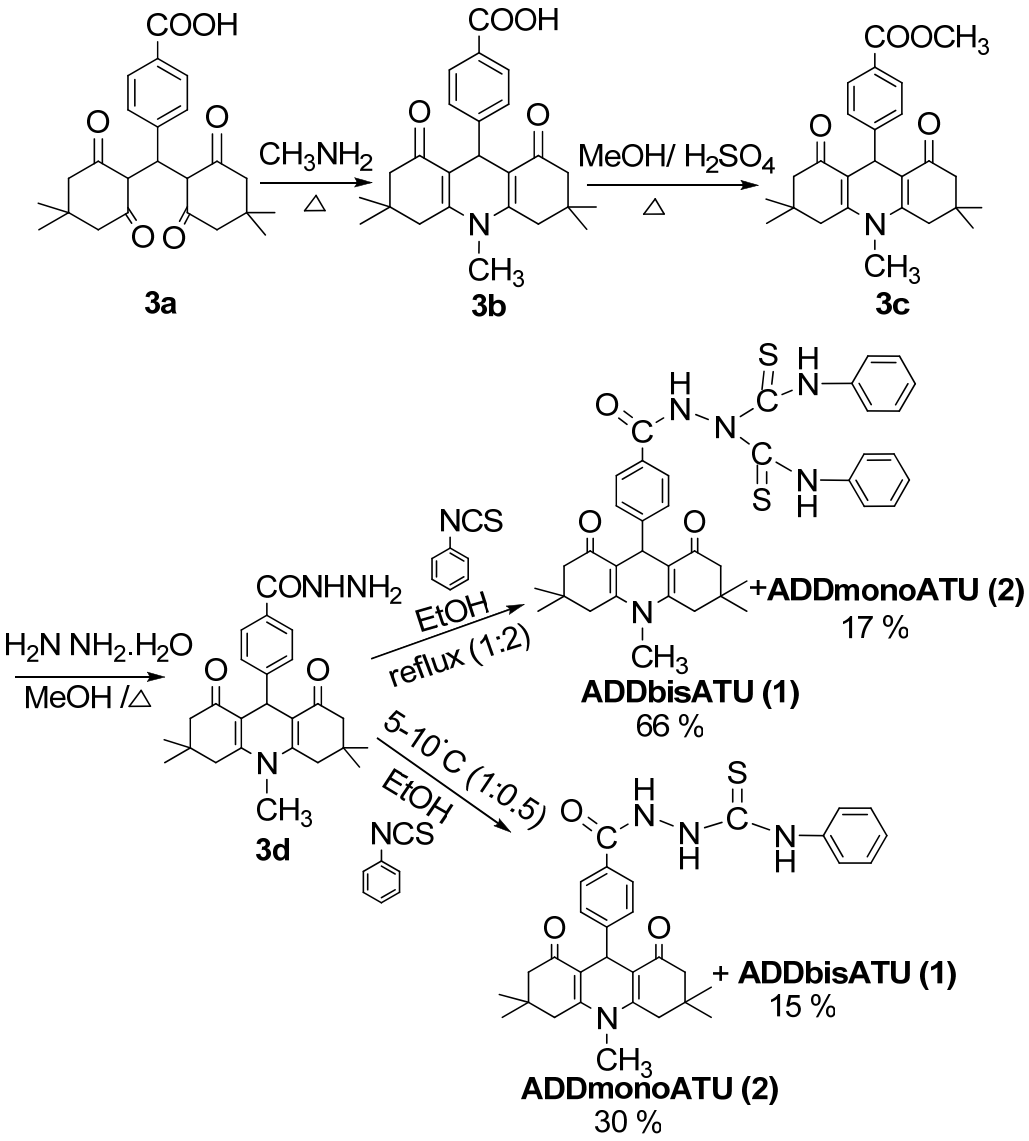

Scheme 1 Synthesis of amidobisthiourea (**1**) and amidothiourea (**2**) derivatives.

To a solution of dimedone (5.0 g, 35.7 mmol) in aq. methanol was added 4-carboxybenzaldehyde (2.67 g, 17.8 mmol) and warmed until the solution became cloudy. The 4-carboxybenzylidine bisdimedone **3a** (6.95 g, 94%) started to

separate out. The reaction mixture was diluted with water and allowed to stand overnight in refrigerator; the tetraketone **3a** was collected by filtration, dried and recrystallised from methanol to yield pure **3a** (6.90 g, 94%) as a colorless powder. M.p. 199-201º C.

A mixture of tetraketone **3a** (2.0 g, 4.85 mmol) and methylamine (40% solution, 0.42 ml, 4.85 mmol) was kept under reflux in acetic acid (20 ml) for 6 hours. After the completion of the reaction, as indicated by TLC, the reaction mixture was cooled and poured into crushed ice. The solid obtained was purified by recrystallisation from $CHCl_3$: MeOH (95:5), to isolate the ADD-acid **3b** (1.74 g, 88%) as a crystalline yellow solid. M.p. 243-245º C; FTIR (KBr): $\bar{\nu}$ = 3155br (OH), 1718s (acid CO), 1631vs (conj. CO), 1373s (-C=C-) cm^{-1}; ^{1}H NMR (300 MHz; DMSO-d_6): δ(ppm)= 0.93 & 1.01 (2s, 12H, gem-dimethyl), 2.07-2.19 (q, 4H, C_2 & C_7 -CH_2), 2.45 & 2.79 (2d, 4H, J= 17.4 Hz, C_4&C_5 -CH_2), 3.29 (s, 3H, -NCH_3), 5.09 (s, 1H, C_9-H), 7.21 (d, 2H, J= 8.1 Hz, ArH), 7.73 (d, 2H, J= 8.4 Hz, ArH), 12.70 (s, 1H, -OH). ^{13}C NMR (300 MHz; $CDCl_3$: DMSO-d_6, TMS) δ (ppm) = 27.63, 28.28, 31.29, 32.07, 33.28, 39.14, 49.39, 112.17, 127.30, 128.17, 128.97, 150.94, 152.91, 167.19, 194.70. MS (ESI): m/z = 407.60; elemental analysis (%) calcd for $C_{25}H_{29}N_1O_4$ (407.50): C 73.68, H 7.17, N 3.44; found: C 73.75, H 7.19, N 3.42.

ADD-acid **3b** (2.0 g, 4.91 mmol) in methanol (20 ml) and a few drops of con. H_2SO_4 was stirred at room temperature. The reaction mixture was poured into water, the solid obtained was purified by recrystallisation from $CHCl_3$: MeOH (97:3, v/v), to isolate ADD-ester **3c** (1.80 g, 87%) as a yellow solid. M.p. 222-224º C; FTIR (KBr): $\bar{\nu}$ = 1699s (ester CO), 1633vs (conj. CO), 1377s (-C=C-) cm^{-1}; ^{1}H NMR (300 MHz; DMSO-d_6): δ(ppm)= 0.92 & 1.0 (2s, 12H, gem-dimethyl), 2.13 (q, 4H, C_2 & C_7 -CH_2), 2.45 & 2.79 (2d, 4H, J= 17.1 & 17.4 Hz, C_4&C_5 -CH_2), 3.29 (s, 3H, -NCH_3), 3.79 (s, 3H, -OCH_3), 5.09 (s, 1H, C_9-H), 7.24 (d, 2H, J= 8.1 Hz, ArH), 7.76 (d, 2H, J= 8.4 Hz, ArH). ^{13}C NMR (300 MHz; $CDCl_3$: DMSO-d_6, TMS) δ (ppm) = 27.56, 28.30, 31.37, 32.05, 33.28, 39.22,

49.35, 51.86, 112.07, 127.07, 127.49, 128.82, 151.39, 152.95, 166.11, 194.69. MS (ESI): m/z = 421.58; elemental analysis (%) calcd for $C_{26}H_{31}N_1O_4$ (421.53): C 74.08, H 7.41, N 3.32; found: C 74.07, H 7.43, N 3.31.

ADD-ester **3c** (1.5g, 3.56 mmol) and hydrazine monohydrate (99%) (0.18 ml, 3.70 mmol) in MeOH (20 ml) was kept under reflux for 14 hours. After the completion of the reaction, as indicated by TLC, the reaction mixture was cooled and poured into crushed ice. The solid obtained was purified by column chromatography over silica gel and eluting with $CHCl_3$: MeOH (95:5, v/v) to isolate the pure ADD-hydrazide **3d** (1.11 g, 74%), as a brown powder. M.p. 190-192º C; FTIR (KBr): $\bar{\nu}$ = 3425b (NH), 1631vs (conj. CO), 1565 (amide CO), 1374s (-C=C-) cm^{-1}; ^{1}H NMR (500 MHz; DMSO-d_6): δ(ppm)= 0.94 & 1.09 (2s, 12H, gem-dimethyl), 2.13 (q, 4H, C_2 & C_7 -CH_2), 2.44 & 2.79 (2d, 4H, J= 17.5 & 17.0 Hz, C_4&C_5 -CH_2), 3.29 (s, 3H, -NCH_3), 5.06 (s, 1H, C_9-H), 7.15 (d, 2H, J= 8.5 Hz, ArH), 7.59 (d, 2H, J= 8.5 Hz, ArH), 9.60 (s, 1H, -NH, D_2O exchangeable). ^{13}C NMR (300 MHz; $CDCl_3$: DMSO-d_6, TMS) δ (ppm) = 27.44, 28.14, 31.06, 32.01, 33.27, 39.17, 49.22, 112.23, 126.01, 127.12, 128.17, 149.11, 153.43, 195.56. MS (ESI): m/z = 421.47; elemental analysis (%) calcd for $C_{25}H_{31}N_3O_3$ (421.53): C 71.23, H 7.41, N 9.97; found: C 71.27, H 7.42, N 9.93.

At low temperature

A solution of ADD-hydrazide **3d** (0.5 g, 1.19 mmol) and phenyl isothiocyanate (0.07 ml, 0.58 mmol) in ethanol (15 ml) was stirred at 5-10˚C for 45 min. After evaporating the solvent, the crude product was chromatographed over a silica gel column and eluted with $CHCl_3$: MeOH (97:3, v/v) to separate pure ADD-monoamidothiourea **2** (0.20 g, 30%) and ADD-bisamidothiourea **1** (0.12 g, 15%).

At refluxing condition

A solution of ADD-hydrazide **3d** (0.5 g, 1.19 mmol) and phenyl isothiocyanate (0.28 ml, 2.34 mmol) in ethanol (15 ml) was kept under reflux for 2 hr. After evaporating the solvent, the crude product was chromatographed over a

silica gel column and eluted with $CHCl_3$: MeOH (97:3, v/v) to separate pure ADD-bisamidothiourea **1** (0.54 g, 66%) and ADD-monoamidothiourea **2** (0.11 g, 17%).

ADDmonoATU (2)

Yellow powder. 186-188º C; FTIR (KBr): $\bar{\nu}$ = 3448b (NH), 1635vs (conj. CO), 1383s (-C=C-) cm^{-1}; ^1H NMR (500 MHz; DMSO-d_6): δ(ppm)= 0.93 & 1.01 (2s, 12H, gem-dimethyl), 2.06-2.18 (2d, 4H, J= 16.0 & 16.5 Hz, C_2 & C_7 -CH_2), 2.45 & 2.79 (2d, 4H, J= 17.5 & 17.0 Hz, C_4&C_5 -CH_2), 3.29 (s, 3H, -NCH_3), 5.07 (s, 1H, C_9-H), 7.14 (t, 1H, ArH), 7.21 (d, 2H, J= 8.5 Hz, ArH), 7.31 (t, 2H, ArH), 7.41 (m, 2H, ArH), 7.75 (d, 2H, J= 8.0 Hz, ArH), 9.64 (s, 1H, -NH, D_2O exchangeable), 9.76 (s, 1H, -NH, D_2O exchangeable), 10.38 (s, 1H, -NH, D_2O exchangeable) ^{13}C NMR (300 MHz; $CDCl_3$: DMSO-d_6, TMS) δ (ppm) = 27.35, 28.05, 28.21, 28.38, 30.69, 31.99, 33.20, 37.05, 40.31, 49.44, 109.83, 110.73, 123.18, 124.89, 126.95, 127.50, 128.75, 130.79, 138.33, 149.64, 150.57, 152.22, 165.85, 174.89, 194.18. MS (ESI): m/z =556.68; elemental analysis (%) calcd for $C_{32}H_{36}N_4O_3S_1$ (556.72): C 69.04, H 6.52, N 10.06; found: C 69.07, H 6.51, N 10.03.

ADDbisATU (1)

Yellow powder. 180-182º C; FTIR (KBr): $\bar{\nu}$ = 3450b (NH), 1648vs (conj. CO), 1384s (-C=C-) cm^{-1}; ^1H NMR (500 MHz; DMSO-d_6): δ(ppm)= 0.82, 1.00 & 1.04 (3s, 12H, gem-dimethyl), 1.98-2.15 (2d, 2H, J= 16 Hz, C_2 & C_7 -CH_2), 2.37-2.44 (ABq, 4H, C_2 or C_7 & C_4 or C_5 –CH_2), 2.65-2.74 (2d, 2H, J= 17 Hz, C_4 & C_5 -CH_2), 3.29 (s, 3H, -NCH_3), 5.27 (s, 1H, C_9-H), 7.13 (t, 1H, ArH), 7.21 (t, 1H, ArH), 7.31 (m, 4H, ArH), 7.42, (m, 4H, ArH), 7.59 (d, 2H, J= 7.5 Hz, ArH), 7.75 (d, 2H, J= 8 Hz, ArH), 9.33 (s, 1H, -NH, D_2O exchangeable), 9.67 (s, 1H, -NH, D_2O exchangeable), 9.73 (s, 1H, -NH, D_2O exchangeable), 10.38 (s, 1H, -SH, D_2O exchangeable), 10.56 (s, 1H, -SH, D_2O exchangeable). ^{13}C NMR (500 MHz; DMSO-d_6, TMS) δ (ppm) = 27.82, 28.41, 28.81, 28.97, 31.18, 32.45, 33.71, 34.26, 37.55, 39.25, 49.95, 110.42, 111.21, 123.76, 125.41, 126.30, 127.47, 128.16,

129.03, 130.40, 138.89, 139.71, 144.17, 150.82, 151.13, 152.65, 166.15, 175.43, 194.57. MS (ESI): m/z = 691.83; elemental analysis (%) calcd for $C_{39}H_{41}N_5O_3S_2$ (691.90): C 67.70, H 5.97, N 10.12; found: C 67.75, H 5.99, N 10.10.

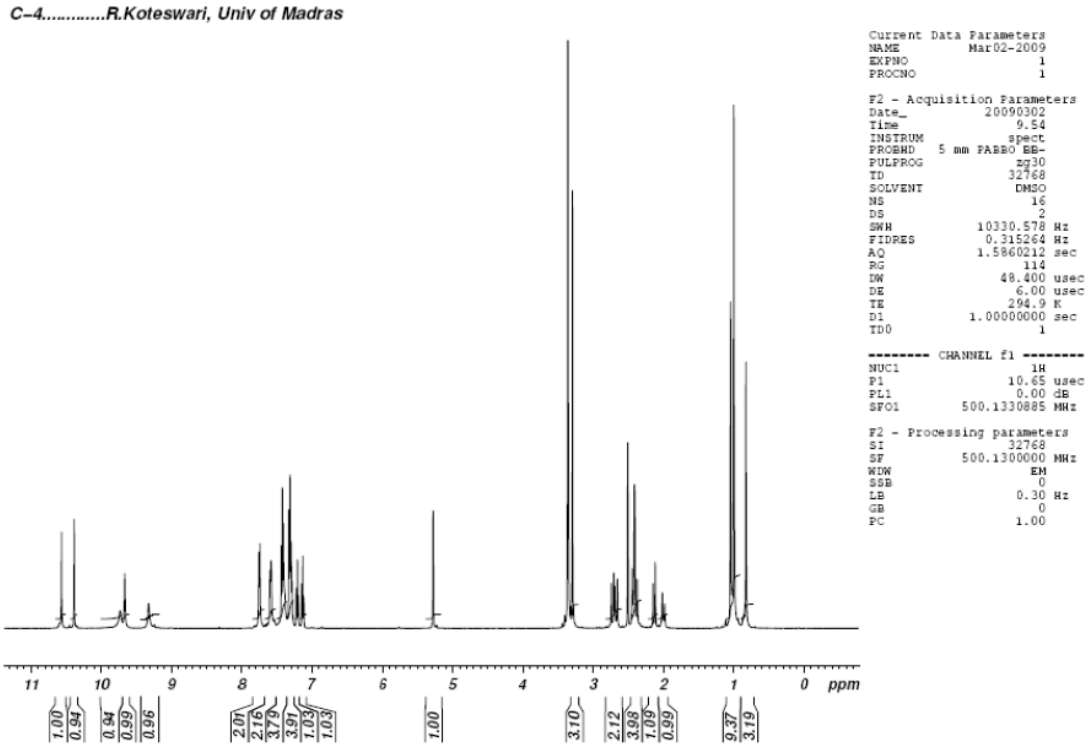

Fig. S1 ^{1}H-NMR spectrum of **1** in DMSO-d_6.

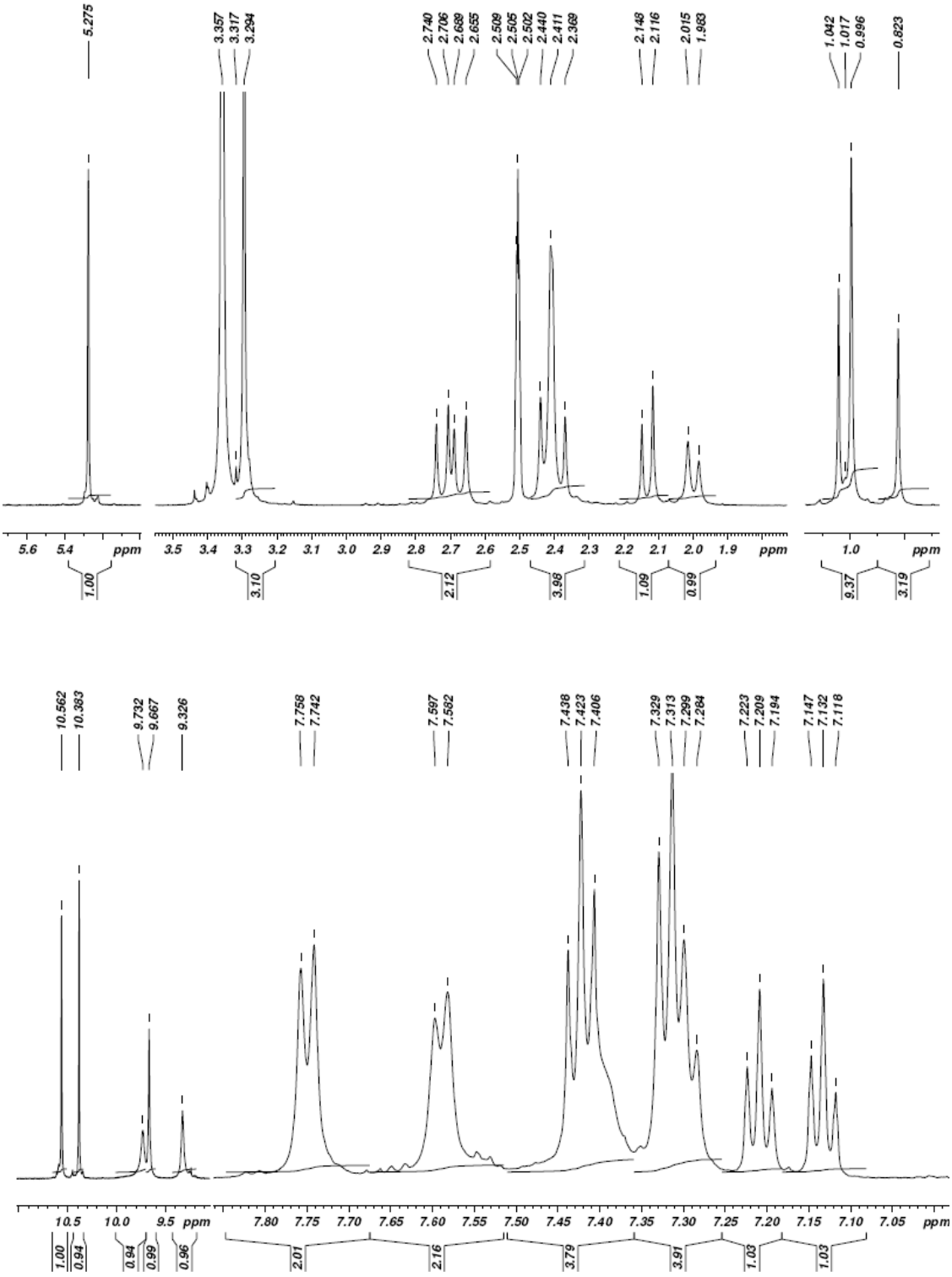

Fig. S2 ^{1}H-NMR (expanded region) of **1** in DMSO-d_6.

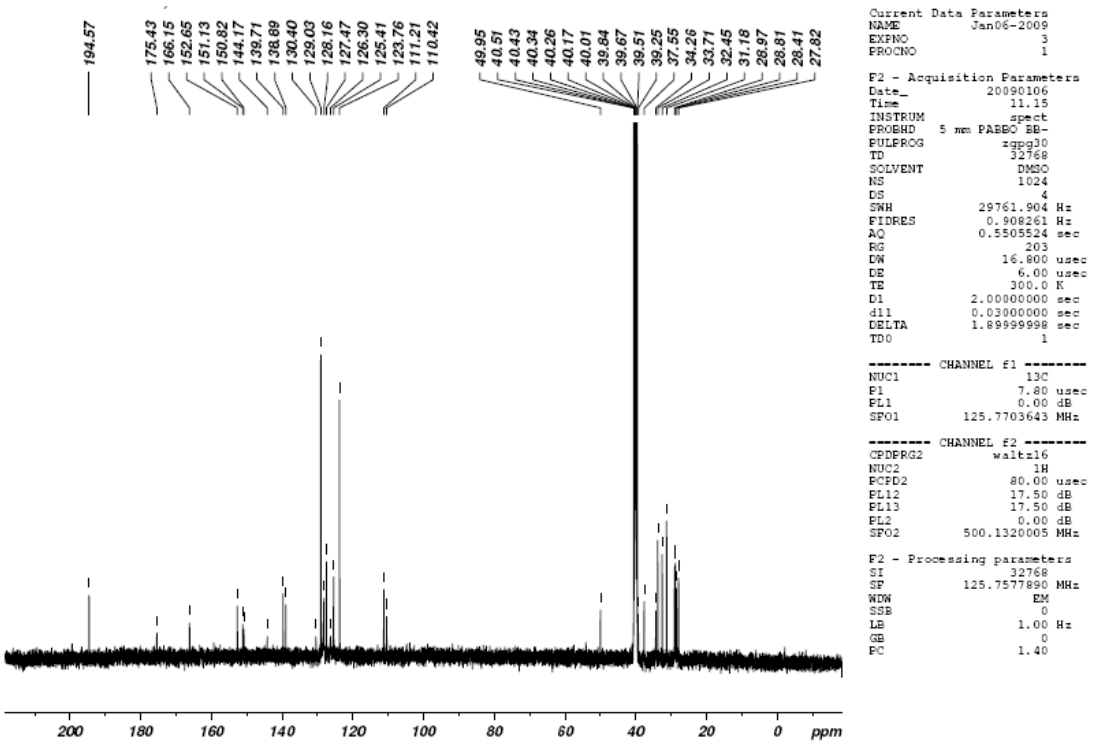

Fig. S3 ^{13}C-NMR of **1** in DMSO-d_6.

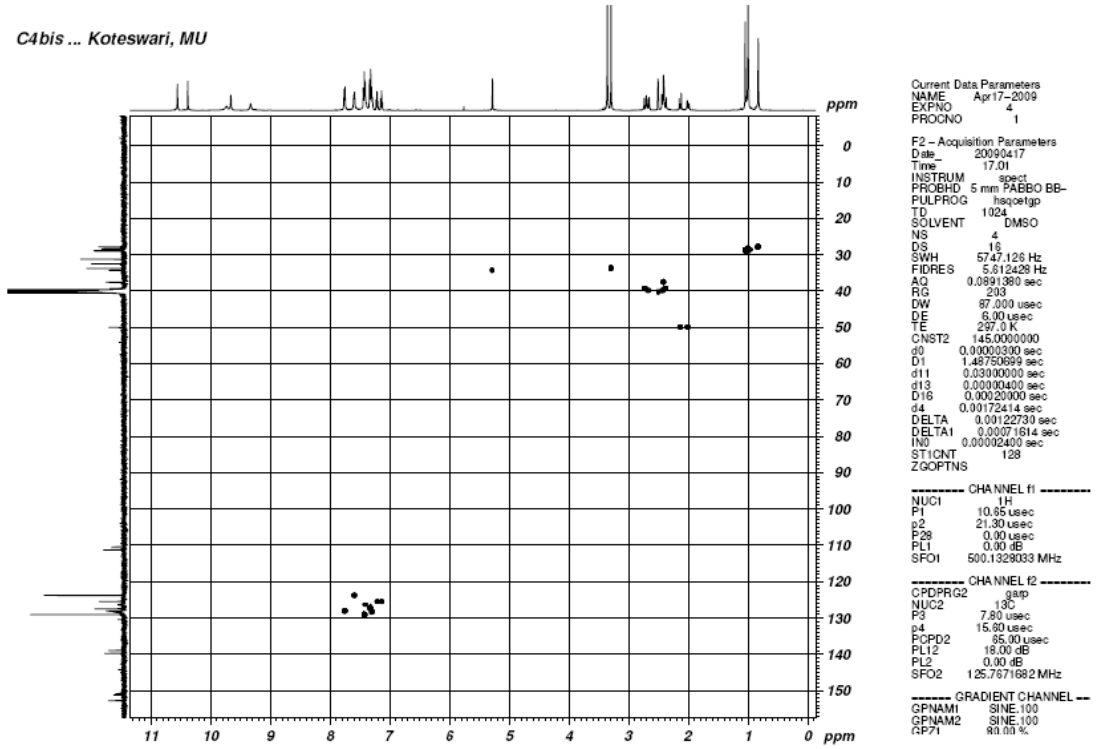

Fig. S4 HSQC spectrum of **1** in DMSO-d_6.

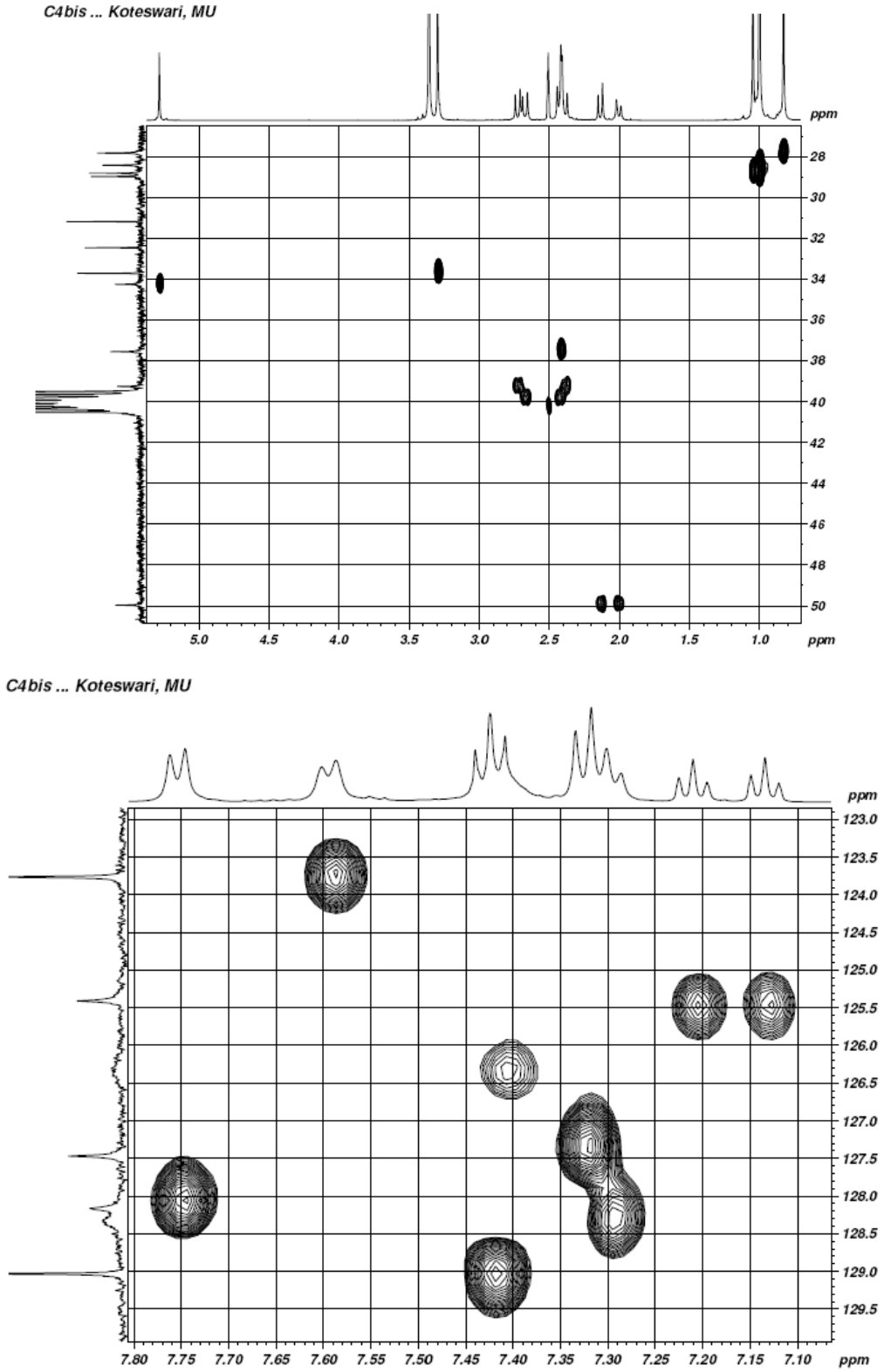

Fig. S5 HSQC spectrum (expanded region) of **1** in DMSO-d_6.

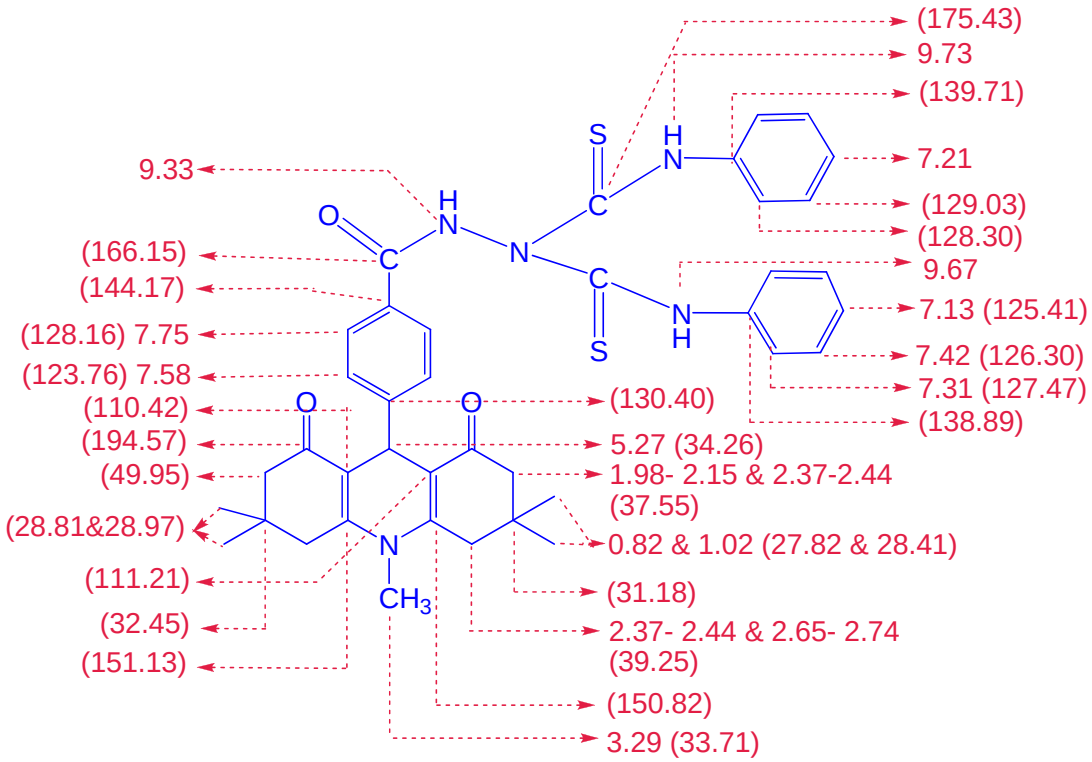

Fig. S6 NMR peak assignment of **1**.

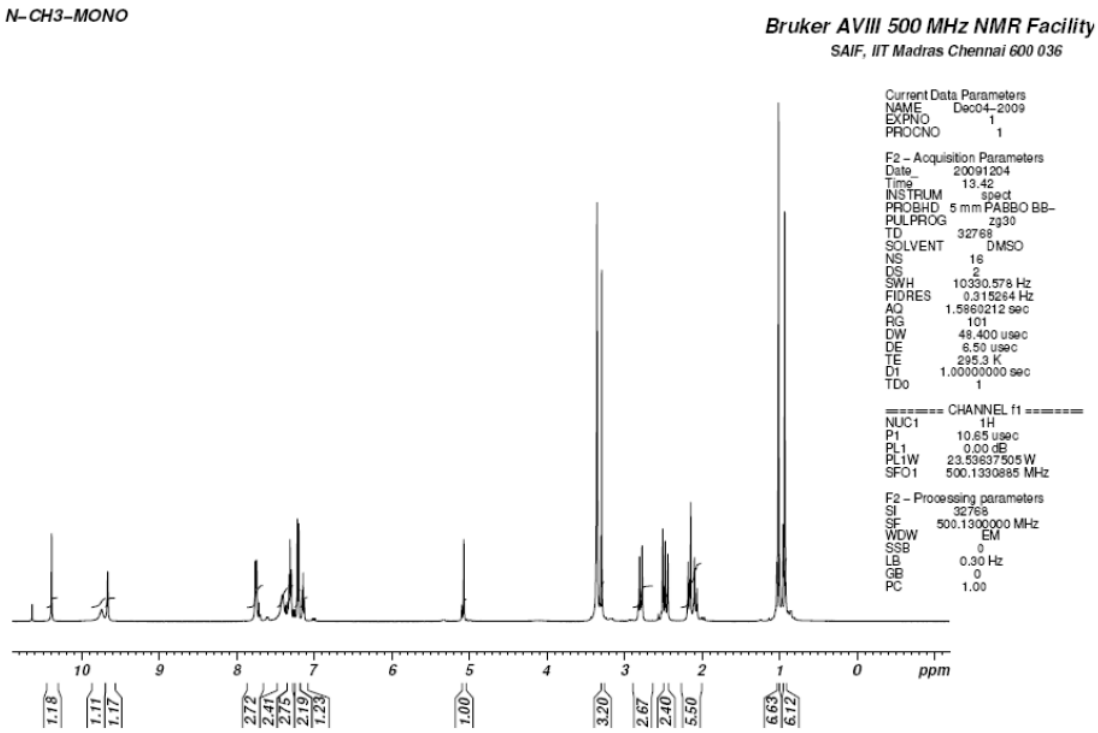

Fig. S7 ^{1}H-NMR spectrum of **2** in DMSO-d_6.

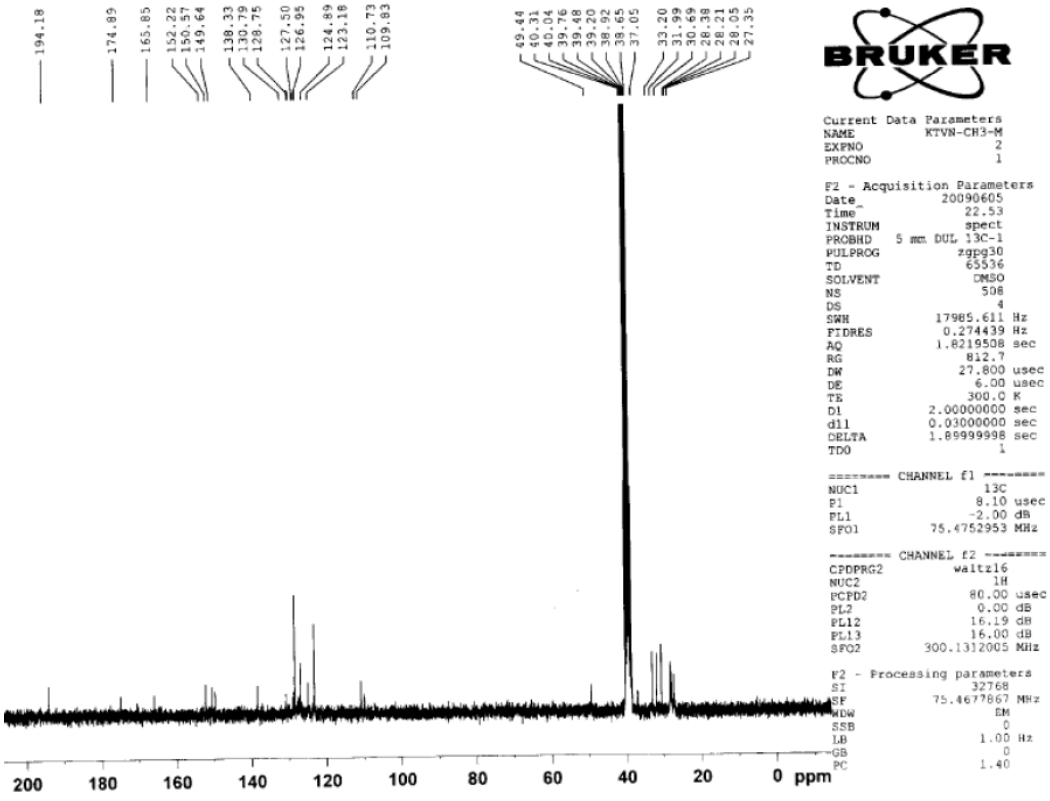

Fig. S8 ^{13}C-NMR spectrum of **2** in DMSO-d_6.

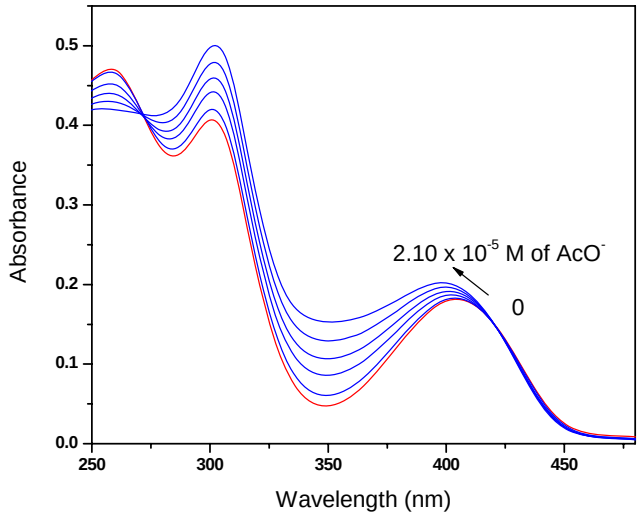

Fig.S9 Absorption spectrum of **1** (16 μM) in acetonitrile upon addition of AcO^- (0-21 μM).

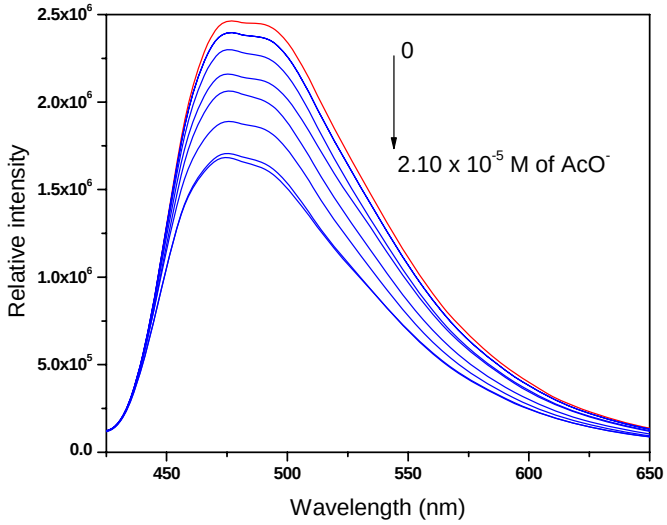

Fig.S10 Emission spectrum of **1** (16 μM) in acetonitrile upon addition of AcO^- (0-21 μM); λ_{ex}= 421 nm.

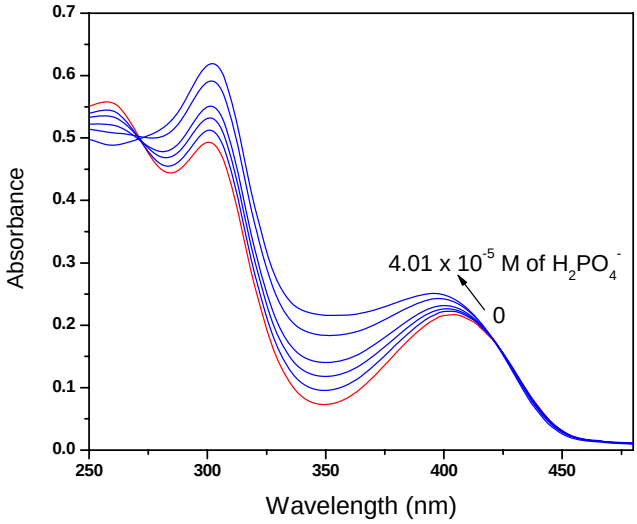

Fig.S11 Absorption spectrum of **1** (20 μM) in acetonitrile upon addition of $H_2PO_4^-$ (0- 33 μM).

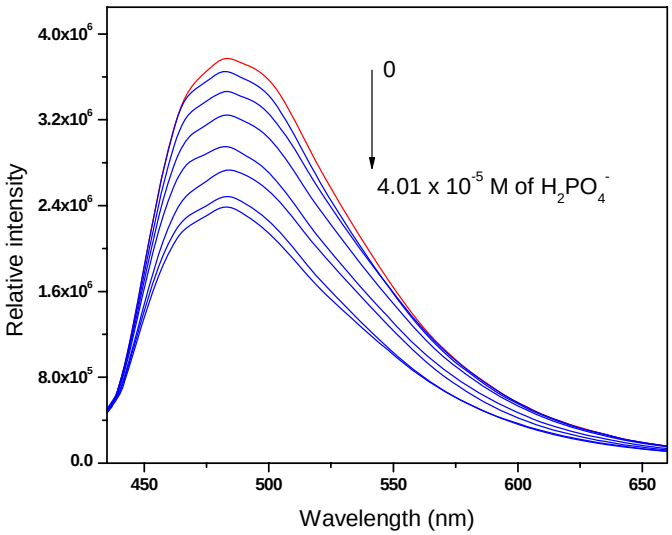

Fig.S12 Emission spectrum of **1** (20 μM) in acetonitrile upon addition of $H_2PO_4^-$ (0- 40 μM); λ_{ex}= 421 nm.

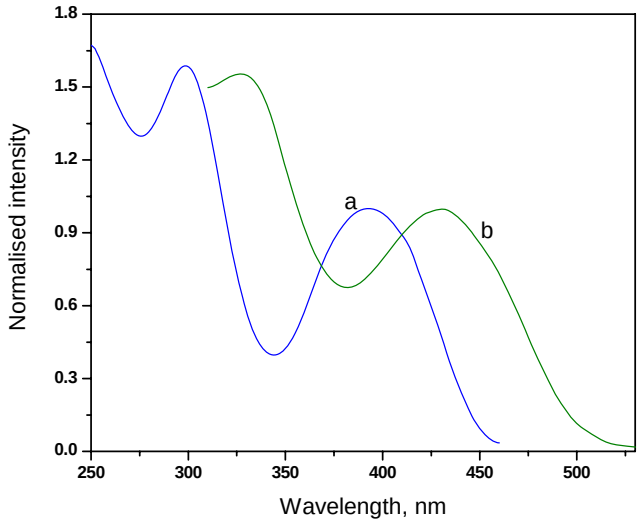

Fig.S13 Excitation spectrum of a) **1** (16 μM), λ_{em} monitored at 480 nm; b) **1**+ F^- (0.73 mM), λ_{em} monitored at 600 nm, in acetonitrile.

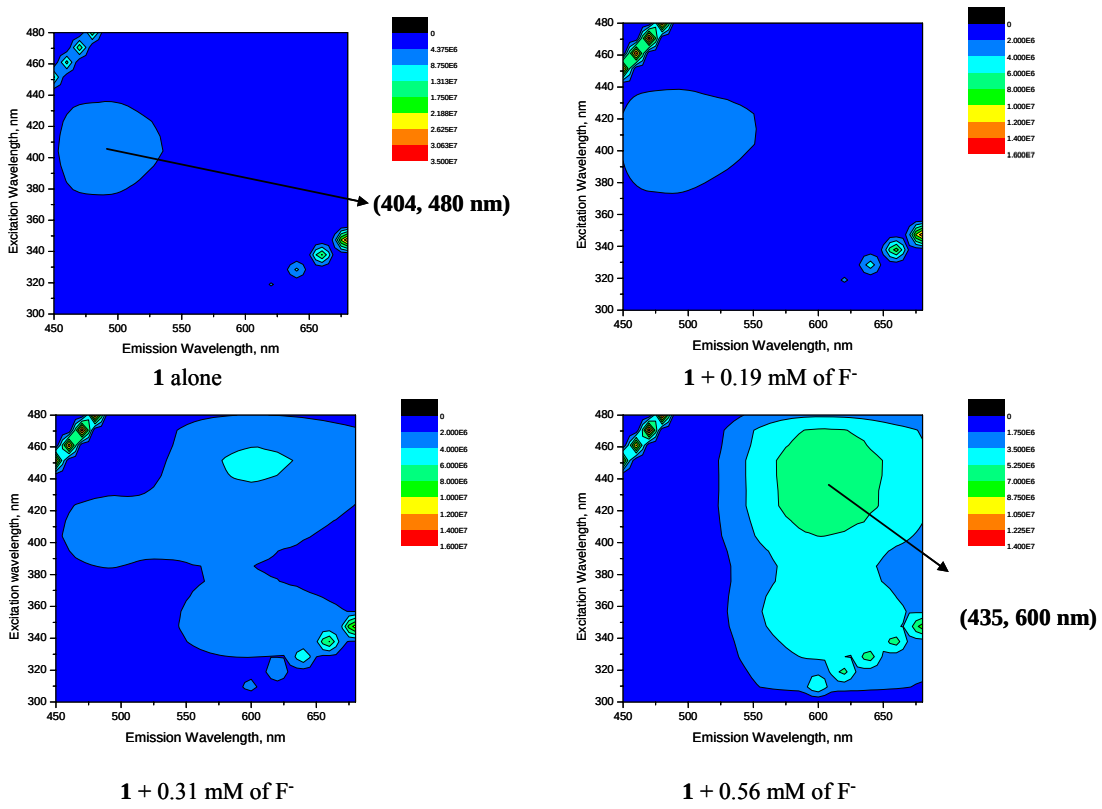

Fig.S14 3D contour spectra of **1** & **1**+ F^- in acetonitrile.

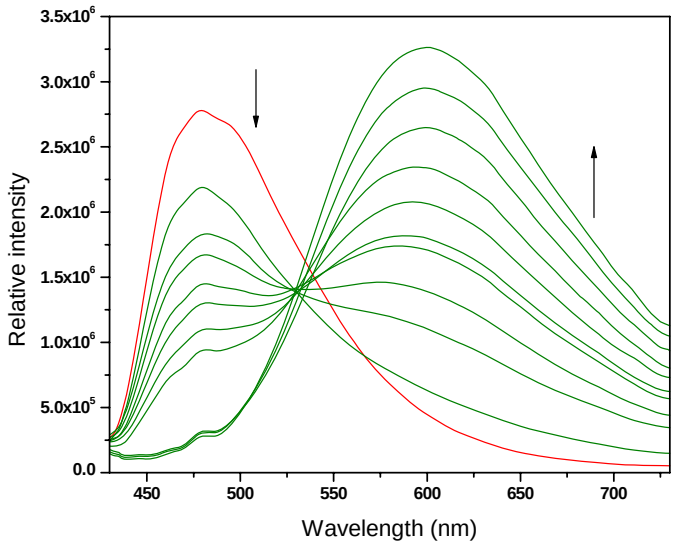

Fig. S15 Emission spectra of **1** (16 μM) in acetonitrile upon addition of OH^- (0-0.58 mM); λ_{ex}= 421 nm.

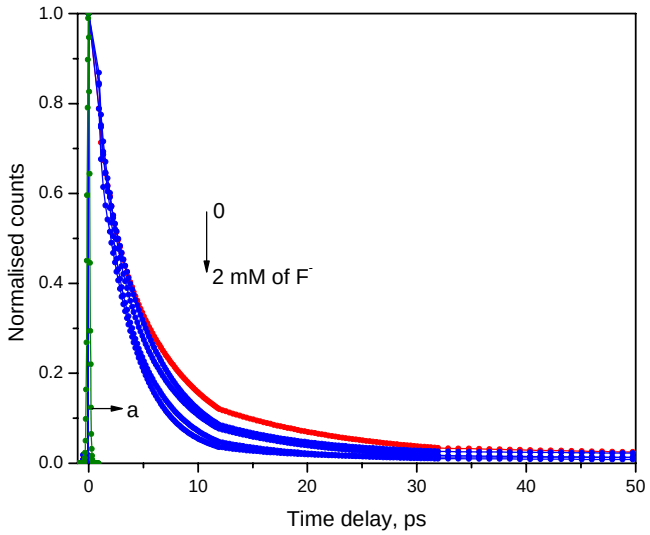

Fig. S16 Femtosecond fluorescence decay of **1** (0.16 mM) in acetonitrile upon addition of F^- (0- 2.0 mM); λ_{ex}= 400 nm; λ_{em}= 480 nm; a) instrument response function.

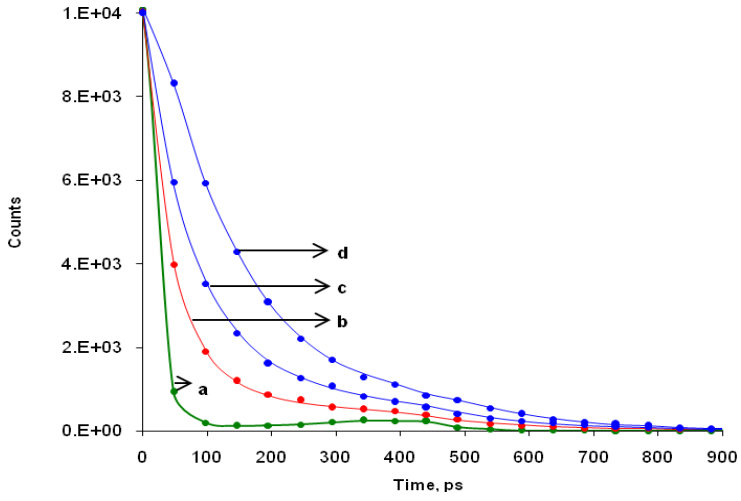

Fig. S17 Fluorescence decay (recorded in TCSPC) of **1** (16 μM) in acetonitrile upon addition of F^-; λ_{ex}= 420 nm; λ_{em}= 600 nm; a) lamp profile; b) **1** alone; c) 0.35 mM; d) 0.75 mM of F^-.

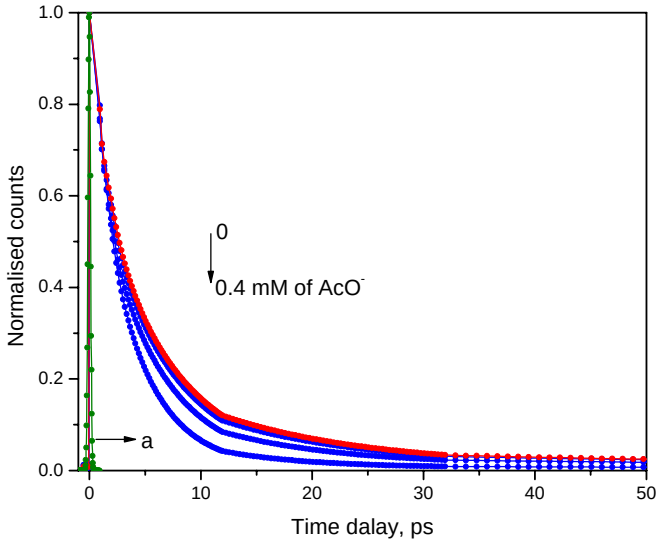

Fig. S18 Femtosecond fluorescence decay of **1** (0.16 mM) in acetonitrile upon addition of AcO^- (0-0.4 mM); λ_{ex}= 400 nm; λ_{em}= 480 nm; a) instrument response function.

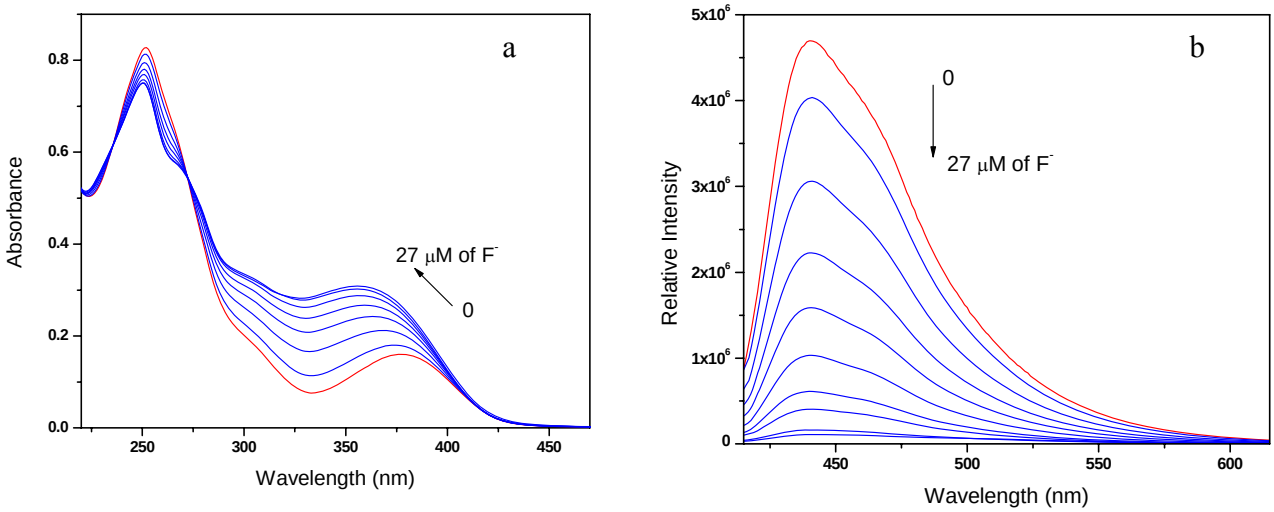

Fig.S19 a) Absorption; b) Emission spectrum of **2** (18 μM) in acetonitrile upon addition of F^- (0- 27 μM); λ_{ex}= 405 nm.

Compound	Abs. max (nm)	Emi. max (nm)	Quantum yield (ϕ_f)[a]	Lifetime (τ_f) (ns)
ADD-acid (**3b**)	376	440	0.70	8.84
ADD-ester (**3c**)	376	440	0.72	9.00
ADD-hydrazide (**3d**)	377	440	0.70	8.84
ADD-monoamidothiourea (**2**)	377	440	0.66	8.22
ADD-bisamidothiourea (**1**)	404	480	0.005[b]	0.043

[a] Fluorescence quantum yields were determined by exciting the sample at 366 nm using quinine sulfate as the standard (Φ_f = 0.546 in 0.1N H_2SO_4); ± 2%; b) ± 5%

Table S1 Photophysical parameters of **1**, **2, 3b**, **3c**& **3d** in acetonitrile.

Species	Binding constant[a] (K) x10^3 M^{-1}	Fluorescence quantum yield[c] (ϕ_f)	Fluorescence lifetime[d] (τ_f), ps
1 alone	---	0.0052	43 ± 3
1.F^-	4.48[b]	0.0027	25 ± 2
deprotonated **1**	1.70[b]	0.0076	140[e] ± 5
1.AcO^-	5.23	0.0028	25 ± 2
1.$H_2PO_4^-$	4.10	0.0028	28 ± 2

[a] The binding constants of **1** with anions were obtained by nonlinear fitting[1] of the fluorescence intensity at 480 nm against anion concentration; [b] Best fitting of the overall titration data was obtained by assuming the existence of two stepwise equilibria, in which (i) **1** interacts with F^- to give [**1.**F^-] and (ii) the [**1**.F^-] complex interacts with another F^-. [c] Fluorescence quantum yields were determined by the above same procedure; ± 5% [d] Fluorescence lifetime were measured from femto upconversion technique (due to very short fluorescence lifetime) by exciting the sample at 400 nm; emission monitored at 480 nm for **1** and its H-bonded complex of anions; [e] Fluorescence lifetime of deprotonated **1** was measured from TCSPC technique by exciting the sample at 420 nm; emission monitored at 600 nm.

Table S2 Fluorescence quantum yield and lifetime of **1** and its anionic complexes in acetonitrile.

Electrochemical characterization

A cyclic voltammetric studies have been carried out in acetonitrile with the addition of anions. Redox active ADD chromophore undergoes irreversible oxidation around 1.0-1.3 V vs Ag/AgCl. The oxidized product undergoes reduction around -1.0 V as reported earlier[2]. The oxidized product strongly adsorbs at the electrode surface, which requires cleaning of the electrodes after each experiment to remove the adsorbed impurities. Compounds **2**, **3b**, **3c**& **3d** show oxidation peak around 1.1-1.2 V, whereas amidobisthiourea derivative **1** shows oxidation peaks at 0.61 & 1.19 V. The peak observed at 1.19 V is attributed to the oxidation of ADD moiety and the peak observed at 0.61 V is of amidobisthiourea moiety. Addition of F^- to **1** did not show any significant change in the oxidation potential of ADD. Since ADD moiety is in non conjugated linking with the receptor site, any variation in the receptor may not influence the redox property of the ADD. In contrast, the oxidation peak of amidobisthiourea moiety shifts towards lower potential due to increased ease of oxidation in the presence of anions. Addition F^- shifts the peak from 0.61 V to 0.05 V (Fig. S20), whereas, AcO^- & $H_2PO_4^-$ shows a shift to 0.50 V.

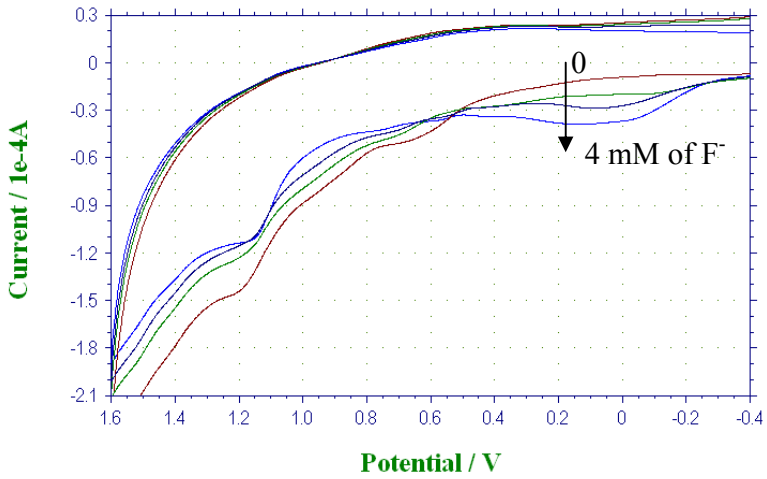

Fig. S20 Cyclic voltammogram of **1** (0.16 mM) with the addition of F^- in acetonitrile. (TBAP (0.1 M) as supporting electrolyte; scan rate 200 $mV.s^{-1}$, vs Ag/AgCl in Ar saturated condition).

Electronic transitions in the excited states

The nature of electronic excitations involved in the low-lying excited states of systems **1**, **1**.F^- and **1**.F_2^{2-} was examined by performing TD-DFT computations using B3LYP functionals and 6-31G* basis set on the B3LYP/6-31+G* optimized ground state geometries. We have invoked all the singly excited configurations generated by single electron excitation from 10 highest occupied MOs to 10 lowest vacant MOs in the TD-B3LYP/6-31G*//B3LYP/6-31+G* computations. Table S3 summarizes the origin of the excitations and the energies of the low-lying states; Fig. S21-23 show the Highest Occupied and Lowest Unoccupied Molecular orbitals of **1**, **1**.F^- (H-bonded complex) & **1**.F_2^{2-} (deprotonated **1**); Fig. S24 represents the schematic energy level diagram of the molecular orbitals involved in the low-lying excited states.

Species	Excited state	Main excitations involved	Configuration -interaction (CI) coefficient	Excitation energy (nm)
1	S1	HOMO → LUMO (HOMO–3) → LUMO (HOMO–2) → LUMO	0.45 -0.39 0.28	410.3
	S2	HOMO → (LUMO+1) (HOMO-3) → (LUMO+1) (HOMO-5) → (LUMO+1) (HOMO-6) → (LUMO+1)	0.43 0.21 -0.39 -0.22	351.2
1.F^-	S1	HOMO → (LUMO+1) (HOMO-2) → (LUMO+1)	0.54 -0.37	382.5
	S2	HOMO → LUMO	0.71	369.2
1.F_2^{2-}	S1	HOMO → LUMO	0.71	469.6
	S2	(HOMO-1) → LUMO	0.71	456.1

Table S3 TD-B3LYP/6-31G*//B3LYP/6-31+G* predicted excitation energies of the low-lying electronic states and the excitations involved in **1**, **1**.F^- & **1**.F_2^{2-}.

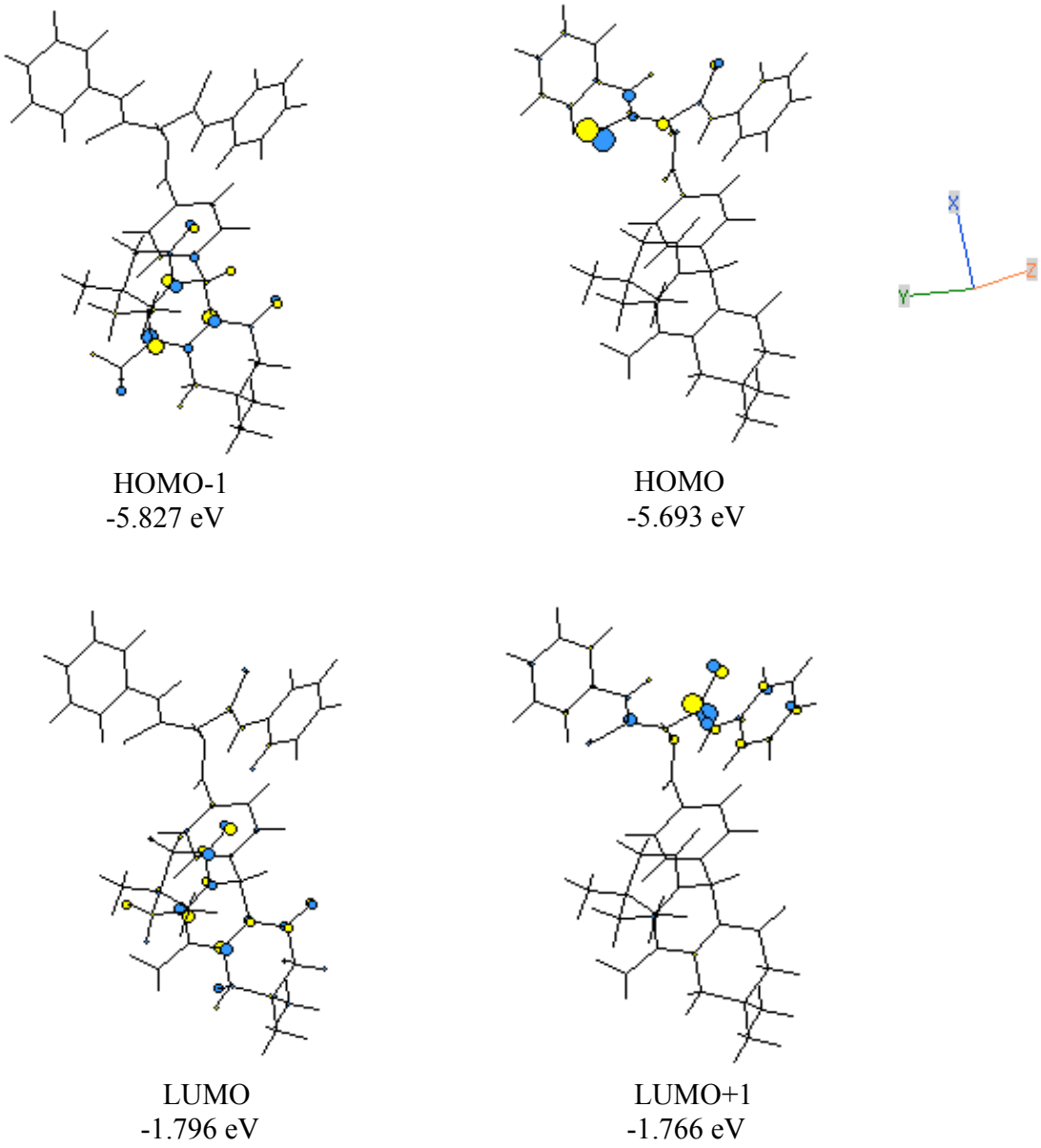

Fig.S21 Highest Occupied and Lowest Unoccupied Molecular Orbitals and their energies (in eV) of **1**.

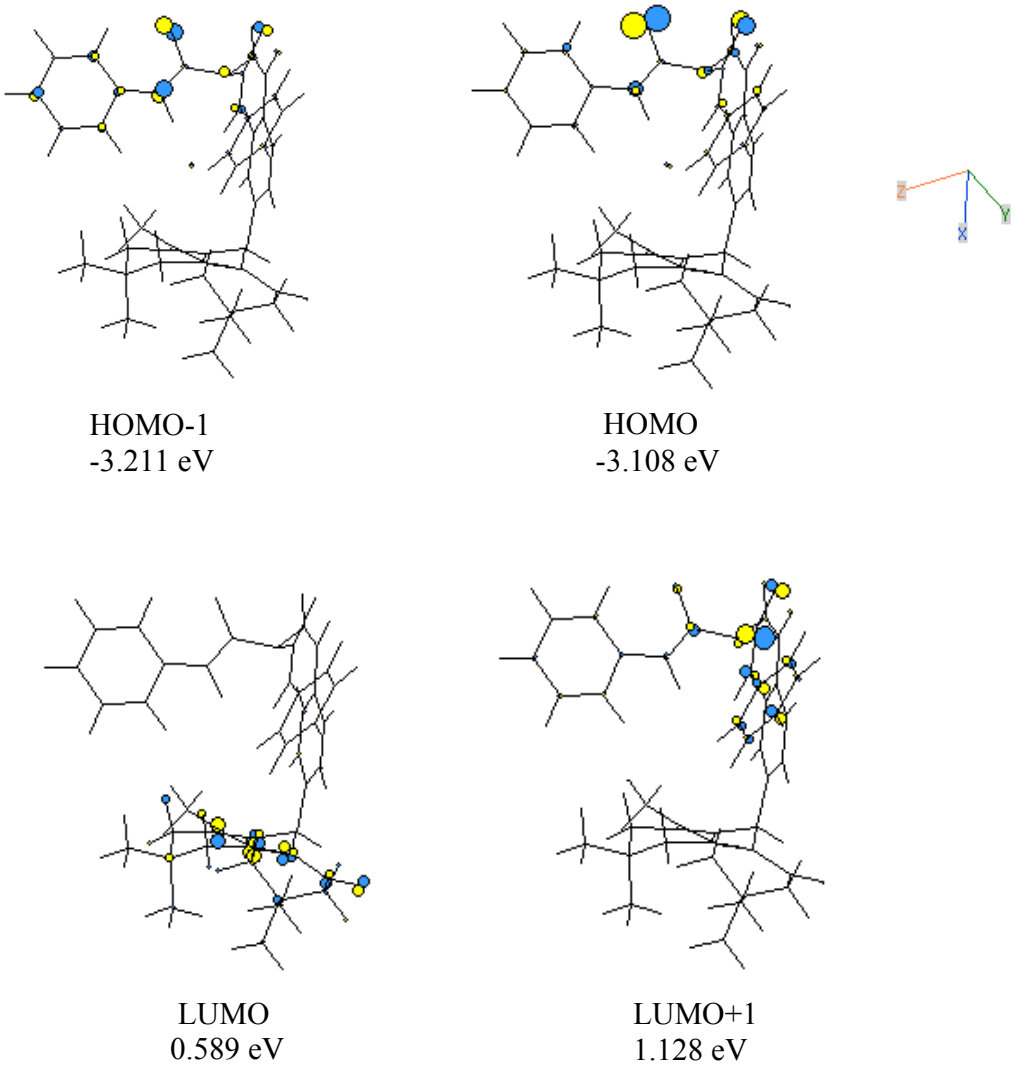

Fig.S22 Highest Occupied and Lowest Unoccupied Molecular Orbitals and their energies (in eV) of **1**.F^- (H-bonded complex).

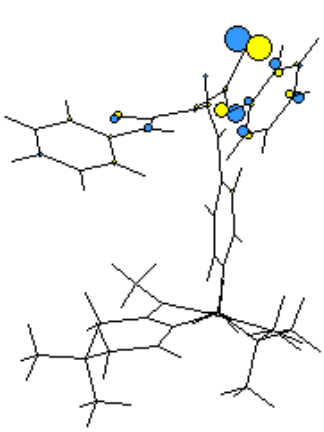

HOMO-1
-0.357 eV

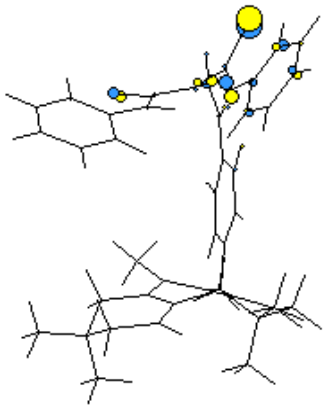

HOMO
-0.282 eV

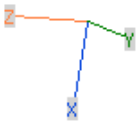

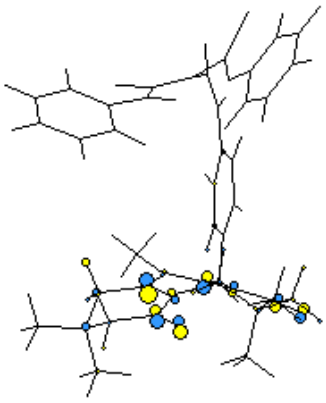

LUMO
2.685 eV

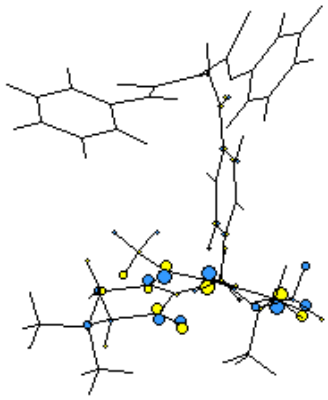

LUMO+1
3.677 eV

Fig.S23 Highest Occupied and Lowest Unoccupied Molecular Orbitals and their energies (in eV) of **1**.F_2^{2-} (deprotonated complex).

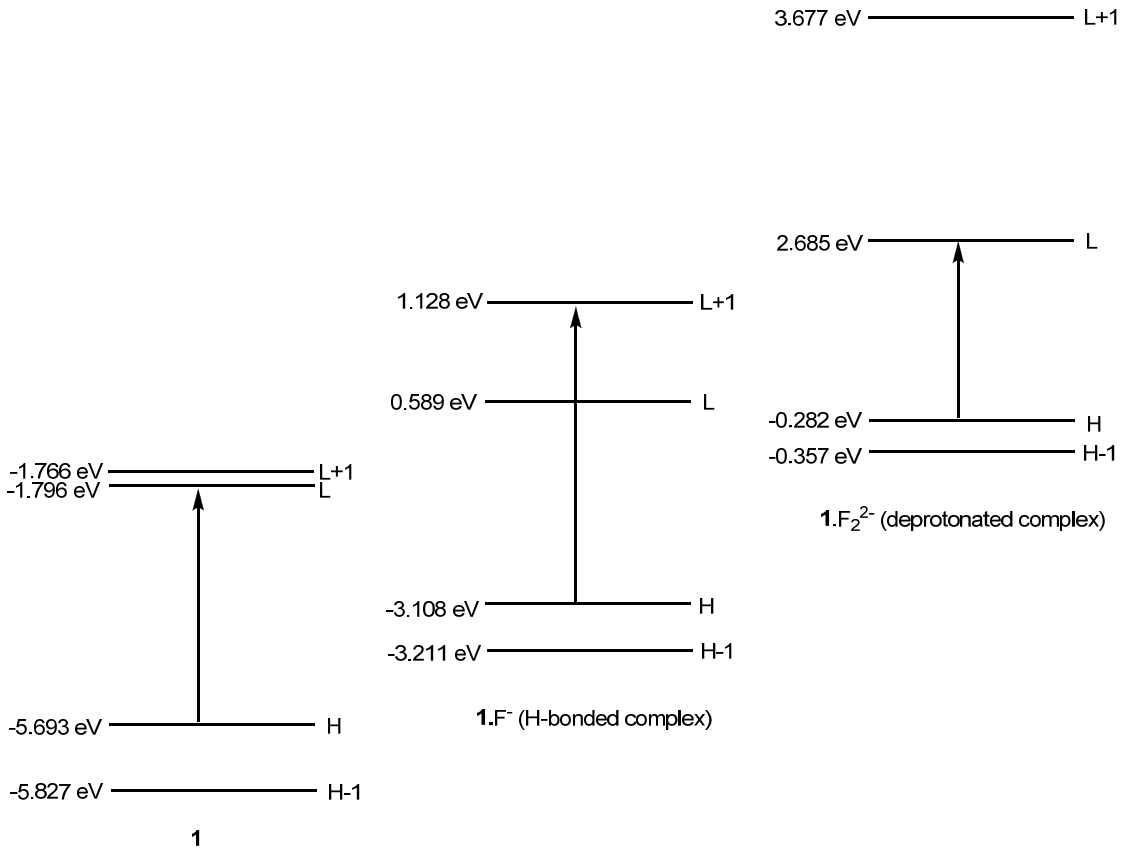

Fig.S24 Schematic representation of molecular orbital energy level diagram of **1**, **1**.F^- (H-bonded complex) and **1**.F_2^{2-} (deprotonated complex).

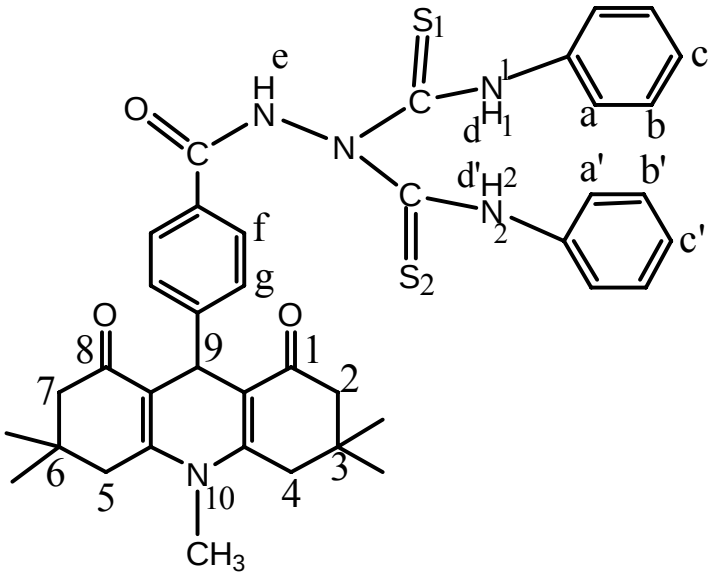

System	H-Bond interaction D-H---A	H-Bond length (A°) H----A	H- bond angles (°) ∠D-H--A
1	$N_2H_2…S_2$	2.869	130.2
	$N_1H_1…O$	2.422	157.0
1.F^- H-bond complex	$N_1H_1…F_1$	1.595	177.6
	$N_2H_2…F_1$	1.583	165.9
	CH a … F_1	2.367	133.5
	CH a'… F_1	2.220	134.7
	$N\text{-}CH_3…F_1$	2.099	158.8
Deprotonated **1** (**1**.F_2^{2-})	$C_4H…F_2$	2.340	134.5
	H_2--- F_2	1.232	175.3
	N_1H_1---N_2	1.814	140.2
	CH a … F_2	2.410	147.5
	CH a'… F_2	2.701	153.2
	$N\text{-}CH_3$--- F_2	2.017	170.3

Table S4 H-bond length & angles of **1**, **1**.F^- & **1**.F_2^{2-}.

Notes and references

1 (a) V. Thiagarajan, P. Ramamurthy, *Spectrochim. Acta. A*, 2007, **67**, 772-777; (b) K. A. Connors, *Binding Constants, The Measurment of Molecular Complex Stability*, John Wiley & Sons, New York, 1987, p. 147.

2 N. Srividya, P. Ramamurthy, P. Shanmugasundaram, V. T. Ramakrishnan, *J. Org. Chem*. 1996, **61**, 5083-5089.